Cardiac Lesion Mapping *In Vivo* Using Intracardiac Myocardial Elastography

Ethan Bunting, Clement Papadacci, Elaine Wan, Vincent Sayseng, Julien Grondin, and Elisa E. Konofagou, *Member, IEEE*

***Abstract*— Radio frequency (RF) ablation of the myocardium is used to treat various cardiac arrhythmias. The size, spacing, and transmurality of lesions have been shown to affect the success of the ablation procedure; however, there is currently no method to directly image the size and formation of ablation lesions in real time. Intracardiac myocardial elastography (ME) has been previously used to image the decrease in cardiac strain during systole in the ablated region as a result of the lesion formation. However, the feasibility of imaging multiple lesions and identifying the presence of gaps between lesions has not yet been investigated. In this paper, RF ablation lesions ($n = 7$) were generated in the left ventricular epicardium in three anesthetized canines. Two sets of two lesions each were created in close proximity to one another with small gaps (1.5 and 4 cm), while one set of two lesions was created directly next to each other with no gap. A clinical intracardiac echocardiography system was programmed to transmit a custom diverging beam sequence at 600 Hz and used to image the ablation site before and after the induction of ablation lesions. Cumulative strains were estimated over systole using a normalized cross-correlational displacement algorithm and a least-squares strain kernel. Afterward, lesions were excised and subjected to tetrazolium chloride staining. Results indicate that intracardiac ME was capable of imaging the reduction in systolic strain associated with the formation of an ablation lesion. Furthermore, lesion sets containing gaps were able to be distinguished from lesion sets created with no gaps. These results indicate that the end-systolic strain measured using intracardiac ME may be used to image the formation of lesions induced during an RF ablation procedure, in order to provide critical assessment of lesion viability during the interventional procedure.**

***Index Terms*— Ablation, elastography, intracardiac, lesion, strain, ultrasound.**

I. Introduction

RADIO frequency (RF) ablation procedures aim to correct various types of arrhythmia by thermally ablating select regions of the cardiac tissue thought to contribute to the abnormal rhythm. Success rates for ablation procedures have been reported in the range of 53%–57% for a single procedure and 71%–80% after multiple procedures [1], [2]. The size, spacing, and depth of the lesions in the tissue have been shown to be critical to the success of an ablation procedure [3]–[6], motivating the development of new methodologies to characterize lesion formation in real time. Conventionally, lesion size has been controlled using temperature, amplitude, and duration of the RF energy provided by the ablation system [7], [8]. Contact force of the ablation catheter has also recently been proposed as a method to control lesion size [9], [10]. However, these methods mainly rely on indirect feedback derived from the ablation catheter instead of direct assessment of myocardial tissue properties and function. As a result, several imaging techniques have been developed to provide more direct mapping of lesion formation within the myocardium. Magnetic resonance imaging [11], [12] has been used to characterize lesion size; however, the specialized equipment and long acquisition times required do not allow real-time monitoring during the procedure. On the other hand, echocardiography has advantages of being fast, low cost, and already highly integrated into the field of interventional cardiology. Intracardiac echocardiography (ICE) is often used during cardiac ablation procedures in order to visualize and monitor the cardiac motion during surgery. The ICE probe may be introduced into the heart using the same route as the ablation catheter, allowing for a convenient imaging view of the ablation site. ICE catheters integrated with high-frequency ultrasound have been used to map lesion formation in real time, using the change in tissue contrast to identify lesion formation [13], [14]. Other ultrasound methods use the fact that stiffening of the cardiac tissue occurs as a result of lesion formation. Shear wave elastography (SWE) uses the shear wave propagation induced by a "push" beam to map tissue stiffness and has been applied to the detection of ablation lesions in beating hearts using an ICE catheter [15]–[18]. Acoustic radiation force imaging (ARFI) also uses an acoustic "push" beam to estimate the displacement at the push location to provide a relative stiffness estimation and was applied to lesion detection in several studies [19], [20]. However, the significant attenuation experienced by the high-frequency probe and by the push beam in the case of SWE and ARFI has thus far required that the imaging transducer to be located within a few centimeters of the lesion. In clinical practice, it may prove challenging to manipulate and align the imaging and ablation catheters in close proximity during the procedure. ICE has also been used for mechanical characterization of the myocardium using strain [21], [22] and strain rate imaging [23], [24].

Manuscript received July 18, 2017; accepted October 27, 2017. Date of publication October 30, 2017; date of current version January 1, 2018. This work was supported in part by the National Institutes of Health Grant EB006042 and Grant HL114358 and in part by the Wallace H. Coulter Foundation. The work of C. Papadacci was supported by the Bettencourt Schueller Foundation. *(Corresponding author: Elisa E. Konofagou.)*

E. Bunting, C. Papadacci, V. Sayseng, and J. Grondin are with the Department of Biomedical Engineering, Columbia University, New York, NY 10027 USA (e-mail: eab2196@columbia.edu).

E. Wan is with the Department of Medicine-Division of Cardiology, Columbia University, New York, NY 10032 USA.

E. E. Konofagou is with the Department of Biomedical Engineering and Department of Radiology, Columbia University, New York, NY 10027 USA (e-mail: ek2191@columbia.edu).

Digital Object Identifier 10.1109/TUFFC.2017.2768301

Recent advancements in plane wave and diverging beam transmissions have been applied to ICE as well [17], [21]. Diverging beam transmissions allow for the simultaneous interrogation of a large field of view, allowing for high frame-rate imaging which has been linked to superior motion and strain estimation [25], [26]. Intracardiac myocardial elastography (ME) has been developed to perform real-time strain imaging using a diverging beam transmission and a fast method of normalized cross-correlation [27]. By taking advantage of the phase of the ultrasound RF data, strain estimation using normalized cross-correlation has been shown to provide for high precision displacement and strain estimation [28], [29]. ME has previously been validated against magnetic resonance tagging and has been used to identify ischemic and infarct regions within the left ventricle (LV) [30], [31]. In regards to cardiac ablation, ME using ICE has previously demonstrated feasibility in detecting the formation of ablation lesions in humans and canines using a clinical ultrasound scanner [21], [32]. However, the use of intracardiac ME to image multiple lesions within the same echocardiographic view has not yet been performed.

In this paper, a large animal ablation study ($n = 3$) with strain estimation using a clinical ultrasound system is described. Using ME, we show that a reduction in strain can be used as a marker for the formation of an RF ablation lesion *in vivo* and that the area affected by the change in strain is correlated with lesion volume. Furthermore, we demonstrate the initial feasibility of ME in monitoring the formation of a lesion line, i.e., multiple lesions placed in close proximity and identifying the presence or absence of gaps between individual lesions. These results further strengthen the role of strain imaging for ablation monitoring and present ME as a potential technique for real-time feedback during clinical procedures.

II. Methods

A. Experimental Setup

Using a protocol approved by the Columbia University Institutional Animal Care and Use Committee, three mongrel dogs weighing approximately 25 kg each were anesthetized using 0.15 mg/kg morphine and sustained under 2%–5% inhaled isoflurane. A lateral thoracotomy procedure was used to expose the heart for placement of the ablation catheter (TactiCath, St. Jude Medical) on the epicardial surface of the LV (Fig. 1). A 6-MHz ICE catheter (ViewFlex, St. Jude Medical) was introduced into the external jugular vein and advanced through the superior vena cava into the right ventricle of the heart, where it was positioned to have a view of the lateral wall of the LV. Alignment between the ICE plane and ablation catheter was achieved by noting the presence of the high reflection produced by the ablation catheter in the standard B-mode image provided by the scanner (green arrow in Fig. 1). The ICE catheter was connected to a clinical ultrasound machine (z.one, Zonare Medical Systems) programmed to emit a specialized sequence for ME imaging which is described in Section II-B.

Ablation lesions were generated at various locations in the epicardium of the LV after confirming alignment between the ablation catheter and ICE view as described above. Seven lesions of different sizes were formed in three dogs using 20 W of power and 20 g of contact force for 60 s each. In two dogs, lesion lines consisting of two lesions were formed having a small gap between lesions (1.5 and 4 cm). Gap distances were defined from the center of each lesion. In one dog, a lesion line was formed with two lesions directly next to each other with no gap in between. Ultrasound acquisitions were performed before and >5 min after the induction of each individual ablation lesion.

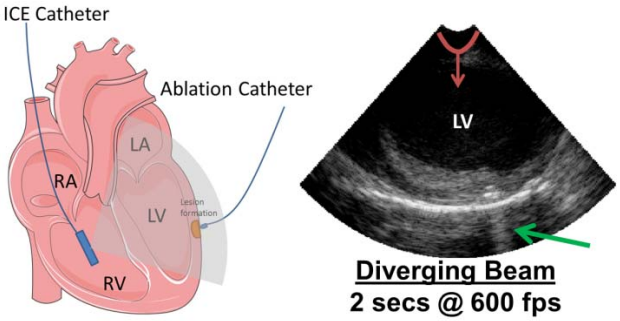

Fig. 1. ICE and ablation catheter placement during experiment. Green arrow indicates position of ablation catheter in ICE view used for alignment.

B. Myocardial Elastography

The ME acquisition sequence was designed for high frame-rate imaging and consisted of repeated diverging wave emissions at 600 Hz at an 11-cm depth for 2 s to ensure capture of the entire cardiac cycle. Each diverging wave contained a focus placed at 6.5 mm behind the probe in order to form a 90° field of view. For each diverging wave, delay-and-sum reconstruction was performed offline using a GPU-accelerated CUDA kernel to reconstruct images at a rate exceeding 500 Hz. The final image stack consists of RF frames containing of 193 lines at a 90° field of view with an axial spatial sampling rate of 18 MHz. ECG measurements were also obtained in synchrony with ultrasound imaging. A fast method for normalized cross correlation was used to estimate 1-D axial displacements for the entire view between consecutive frames (window size = 6.16 mm and overlap = 90%) [27] at a rate exceeding 600 Hz. These interframe displacements were tracked throughout systole and accumulated over time to form Lagrangian cumulative displacements. Axial cumulative strain was derived from the cumulative displacements using a least-squares estimator with a 1-D axial kernel (window size = 0.515 mm). Manual selection of the systolic phase was guided by the ECG and an M-mode image of the displacements of the center line of the image stack [Fig. 2(B)]. The myocardium was segmented manually based on the B-mode image at end diastole.

C. Quantification of Lesion Size

The cumulative end-systolic strain distribution estimated using ME was used to quantify the mechanical changes caused by the ablation lesion and to generate a lesion map. The lesion area was computed to be strains located at the ablation site which were close to zero, defined as between −3% and +3% end-systolic strain. This threshold allowed a visualization of

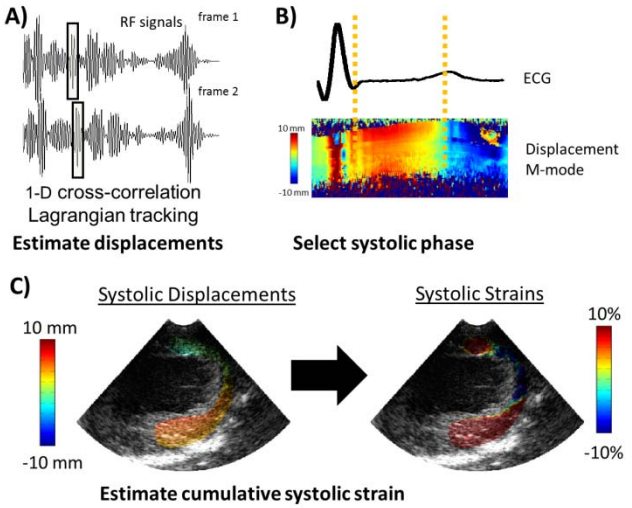

Fig. 2. Description of strain estimation methods. (A) Normalized cross correlation is used to estimate interframe displacements throughout the myocardium. (B) Systole is chosen manually based on the ECG and displacements, allowing for (C) interframe displacements to be accumulated throughout systole and converted to systolic strain using a least-squares estimator.

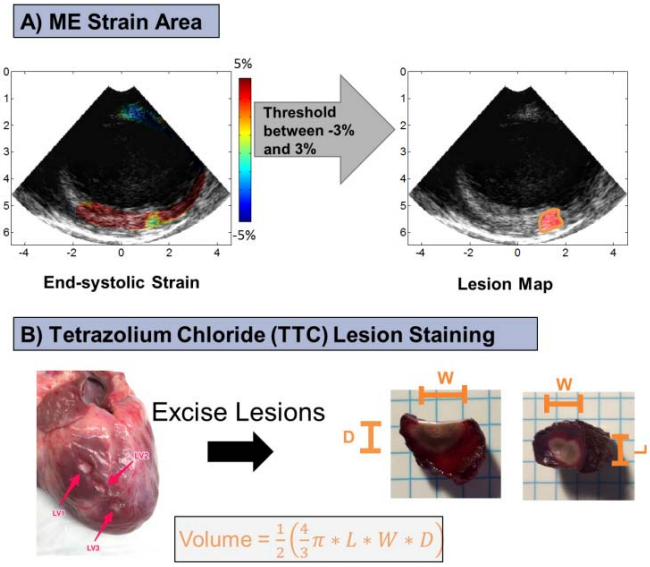

Fig. 3. Methods for determining lesion volume based on strain computed from (A) intracardiac ME and (B) TTC staining.

the lesion area in the region of the image near the ablation location, i.e., a lesion map (Fig. 3). The area of the lesion was computed from the lesion maps as shown in Fig. 3 by counting the number of pixels contained within the thresholded lesion. This area was then compared to the actual lesion volume measured *ex vivo*.

Following the experiment, the lesions were excised from the cardiac tissue and subjected to tetrazolium chloride (TTC) staining and measurement (Fig. 3). Lesion volume was calculated from gross pathology by assuming a half-ellipsoidal shape and measuring the three appropriate axes in the TTC-stained tissue (*L, W,* and *D*) as shown in Fig. 3.

III. Results

Fig. 4 depicts the end-systolic strains and displacements in the LV before and after the application of ablation for a single

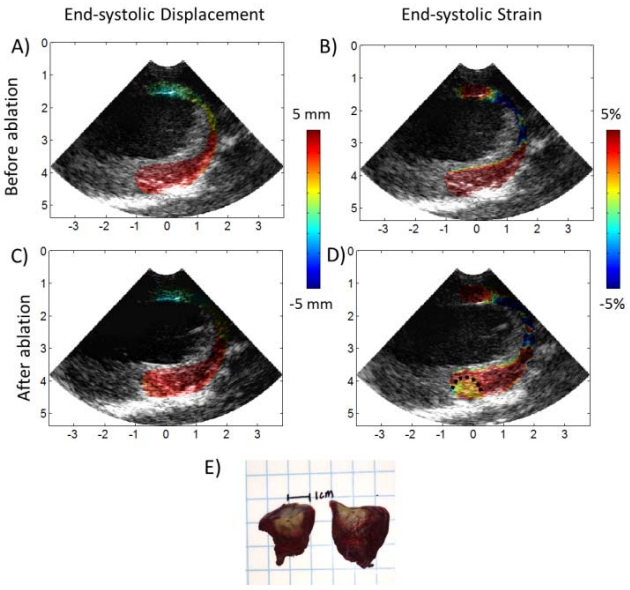

Fig. 4. End-systolic displacement and strain distribution obtained in the canine LV (A) and (C) before ablation and (B) and (D) 5 min after ablation for a single isolated lesion. (E) TTC staining of the excised lesion is performed *ex vivo* to demonstrate the extent of the lesion. Axes units in centimeter.

isolated lesion. Before ablation, end-systolic strain is positive in both the septum (top of image) and lateral wall (bottom of image) in each case. After ablation, a large decrease in strain is observed near the epicardium of the lateral wall. The regions of the myocardium remote from the lesion site also show similar end-systolic strains before and after the ablation. The strain image has been saturated at $\pm 5\%$ strain to indicate the presence of healthy myocardium.

In Fig. 5, the end-systolic strain for the two lesion lines containing no gap is shown. Again, myocardial strain is positive throughout the septal and lateral walls before the formation of the lesions [Fig 5(A)]. Following the formation of the first lesion [Fig. 5(B)], a localized reduction in strain is present in the lateral wall. Following the formation of the second lesion [Fig. 5(C)], this area of strain reduction is increased. Images of the epicardial surface *in vivo* [Fig. 5(D)] and the TTC staining [Fig. 5(E)] confirm that there is no gap present between the two lesions. The size and transmurality of the lesions shown in Fig. 5(C) are also in agreement with the TTC staining.

Figs. 6 and 7 demonstrate the end-systolic strain for the formation of the lesions within the same view containing a gap between them. Following the formation of the first lesion [Figs. 6(B) and 7(B)], a localized reduction in strain is present as shown in Figs. 3 and 4. Following the formation of the second lesion [Figs. 6(C) and 7(C)], a second region of localized strain reduction appears in a region remote from the first. However, positive strain indicative of healthy myocardium persists in the space between the two lesions, identifying the gap that exists between the two lesions. The presence of the gap is confirmed through the image of the epicardial surface [Figs. 6(D) and 7(D)]. The gap shown in Fig. 7(C) (4 cm) is significantly wider compared to Fig. 6(C) (1.5 cm), which is also confirmed by the images of the epicardial surface.

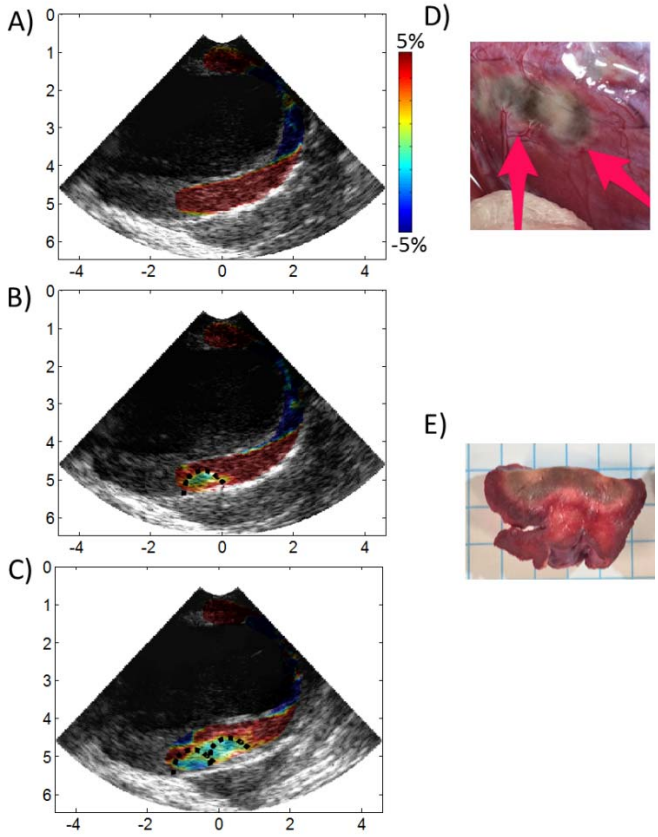

Fig. 5. End-systolic strain distribution obtained in the canine LV after the creation of two lesions without a gap in between. Cumulative end-systolic strain is shown (A) before ablation, (B) 5 min after the creation of the first lesion, and (C) 5 min after the creation of the second lesion. (D) Surface image of the lesion obtained *in vivo* and (E) result of TTC staining of the excised lesions. Epicardial surface is towards the top in (E). Axes units in centimeter.

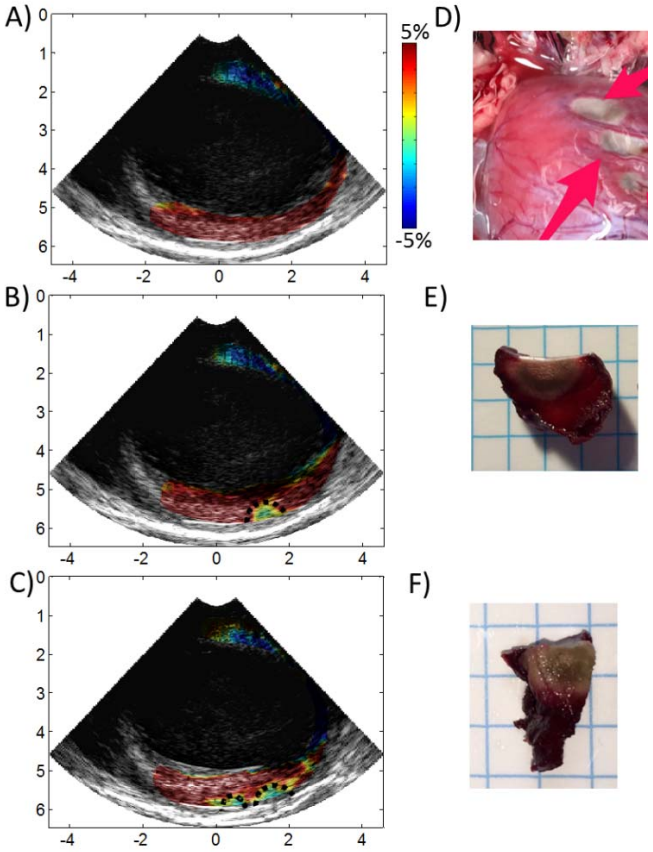

Fig. 6. End-systolic strain distribution obtained in the canine LV after the creation of two lesions containing a 1.5-cm gap in between. Cumulative end-systolic strain is shown (A) before ablation, (B) 5 min after the creation of the first lesion, and (C) 5 min after the creation of the second lesion. (D) Surface image of the lesions obtained *in vivo* and (E) and (F) result of TTC staining of the excised lesions. Epicardial surface is towards the top in (E) and (F). Axes units in centimeter.

A correlation plot between the lesion area measured using ME and lesion volume measured in histology is shown in Fig. 8. The lesions contained within the no-gap set were quantified individually and as a group. A high correlation ($r^2 = 0.91$) was obtained between the lesion maps based on end-systolic strain and histology. Without including the no-gap lesion set as a single lesion in the plot, the correlation was $r^2 = 0.64$.

IV. Discussion

In this paper, we have described a strain-based method, ME, for characterizing the size and location of ablation lesions within the myocardium using a clinical ICE system which can be used during interventional procedures in real time. We have demonstrated that a local reduction in end-systolic strain is associated with the formation of an ablation lesion, thereby allowing for lesion mapping to be performed within the ICE image. Lesion size measured using intracardiac ME was well-correlated with lesion volume as assessed by gross pathology. We have also demonstrated the initial feasibility of detecting gaps between lesions using our technique.

Strain estimated using ME can be used to provide a real-time mechanical characterization of the target region of ablation procedures and the surrounding tissue. Before ablation, cardiac strain is consistently positive throughout the septal and lateral walls, corresponding to the mechanical contraction and thickening that occur throughout systole. As shown in Figs. 4–7, cardiac strain exhibits significant and localized changes following ablation, while remote regions remain relatively unchanged. The magnitude of the strains within each of the lesions is relatively close to zero (between -3% and 3% strain), which is reflective of the increase in stiffness experienced by the tissue following ablation. Proper selection of a threshold to distinguish healthy tissue from ablated tissue is the subject of ongoing study. However, it is clear from the Figs. 4–7 that healthy myocardium consistently experiences $>5\%$ cumulative strain at end systole. Because the mechanical stress experienced by the tissue is unknown, direct mapping of the tissue modulus cannot be obtained. Rather, intracardiac ME aims to use the relative change in end-systolic change experienced by the tissue in real time to identify the formation of localized increases in stiffness indicative of lesion formation.

The widespread use of echocardiography in interventional cardiology is in part related to its low cost, ease of use, portability, and safety. Echocardiographic techniques to provide lesion mapping capabilities have been the topic of several reports in the literature. Unlike radiation force-based techniques, ME exploits the natural contraction of the myocardium

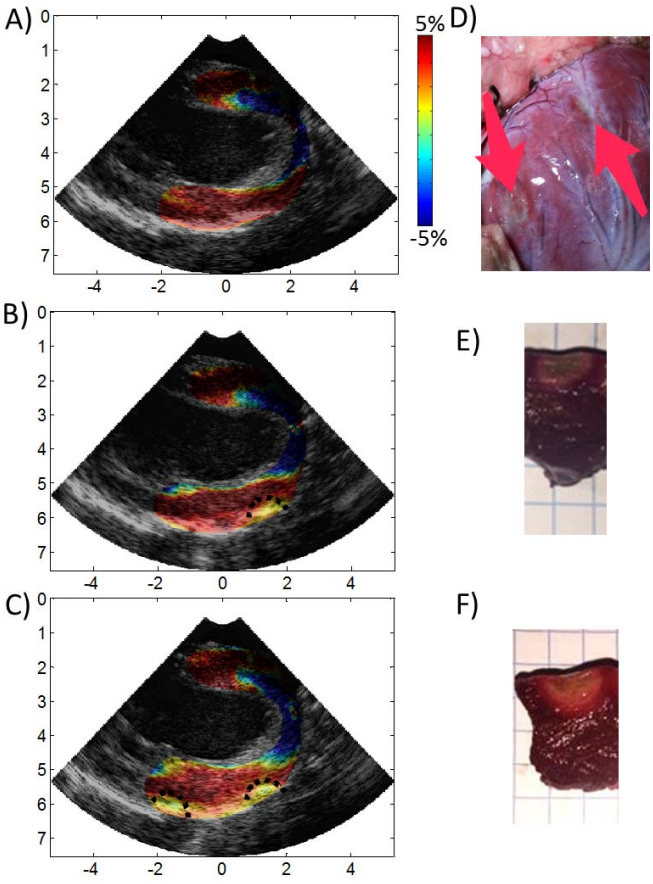

Fig. 7. End-systolic strain distribution obtained in the canine LV after the creation of two lesions containing a 4-cm gap in between. Cumulative end-systolic strain is shown (A) before ablation, (B) 5 min after the creation of the first lesion, and (C) 5 min after the creation of the second lesion. (D) Surface image of the lesions obtained *in vivo* and (E) and (F) result of TTC staining of the excised lesions. Epicardial surface is towards the top in (E) and (F). Axes units in centimeter.

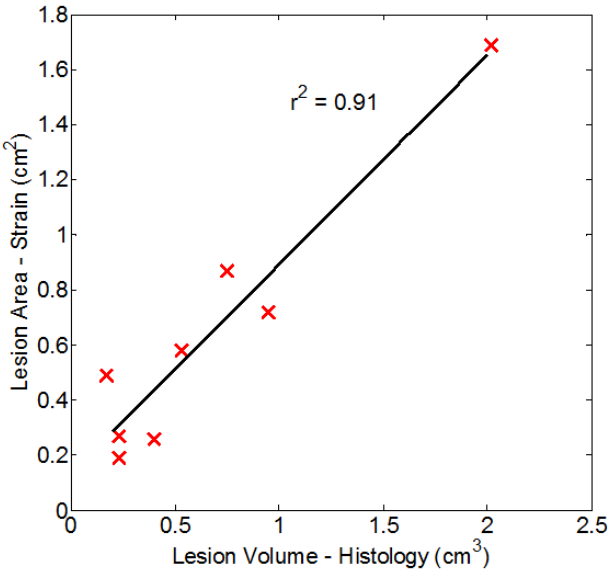

Fig. 8. Correlation between lesion area measured using intracardiac ME and lesion volume assessed by histology.

place of a push beam, rendering direct stiffness mapping more challenging since the tissue stress is unknown. However, ME enjoys other advantages related to the absence of the push beam, namely, high-depth penetration and large field of view. Since ME is not limited by the penetration depth and location of the acoustic push beam, it enables lesion mapping throughout the entire view of the heart within a single cardiac cycle. Furthermore, the location of the lesion does not need to be precisely known before imaging, as long as it is capable of being captured within the ICE view. This may be especially important when imaging multiple lesions or lesion lines, as the transmission settings and ICE view need not be adjusted depending on the location of the ablation site within the image.

Using a diverging beam acquisition, we have achieved an imaging frame rate of 600 Hz to increase the precision of the strain estimation performed by normalized cross correlation. It is well-established that increasing the frame rate is beneficial for axial strain estimation by way of decreasing the interframe axial strains [25], [26]. However, standard diverging beam acquisitions do suffer a tradeoff in spatial resolution, particularly in the lateral direction [33]. Methods such as coherent spatial compounding could be used to increase the spatial resolution in the lateral direction while still maintaining a high frame rate [33], [34]. Future studies should aim to explore the application of coherent compounding to intracardiac imaging and to further characterize the resolution of lesion detection using ME.

As intracardiac ME moves toward implementation of GPU-accelerated hardware, it is expected that fully real-time processing of the end-systolic strain image during the procedure will be feasible. As of now, the processing of the strain estimation pipeline can be performed at >200 Hz; however, fully automated processing is currently impeded by myocardial segmentation, which was performed manually in this paper. Another advantage of intracardiac ME is the fact that the strain estimation processing can be easily extended to 3-D. The use of 3-D imaging would increase the field of view for lesion mapping and eliminate any alignment ambiguities that exist as a result of the imaging plane. Recently, we have demonstrated *ex vivo* and *in vivo* lesion detection using a 2-D matrix array [35], [36]. Intracardiac systems with 2-D matrix array probes have also recently been developed to enable volumetric intracardiac imaging [37], [38].

V. Conclusion

The results of this paper support the use of ME to monitor the formation and assess the size of ablation lesions *in vivo*. As expected, the presence of an ablation lesion within the myocardium leads to decreased end-systolic cumulative strain measured using intracardiac ME. Lesion size assessed using ME is well-correlated with the excised lesion size measured in histology. Furthermore, this paper has demonstrated that gaps between lesions can be detected using this technique. Since ICE imaging already plays an important role in conventional clinical practice during RF ablation procedures, use of imaging techniques such as ME may serve to augment the role of ICE

during ablation procedures and provide a means for lesion visualization, currently absent from the standard of care. The lesion mapping capabilities of ME may serve to increase the success rates of ablation procedures by allowing assessment of the size, spacing, and depth of lesions in real-time during the procedure.

ACKNOWLEDGMENT

The authors would like to thank A. Costet and L. Melki for their help during experiments.

REFERENCES

[1] H. Calkins *et al.*, "Treatment of atrial fibrillation with anti–arrhythmic drugs or radio frequency ablation: Two systematic literature reviews and meta–analyses," *Circulat. Arrhythmia Electrophysiol.*, vol. 2, no. 4, pp. 349–361, Aug. 2009.

[2] A. N. Ganesan *et al.*, "Long-term outcomes of catheter ablation of atrial fibrillation: A systematic review and meta-analysis," *J. Amer. Heart Assoc.*, vol. 2, no. 2, p. e004549, Apr. 2013.

[3] R. Cappato *et al.*, "Prospective assessment of late conduction recurrence across radiofrequency lesions producing electrical disconnection at the pulmonary vein ostium in patients with atrial fibrillation," *Circulation*, vol. 108, no. 13, pp. 1599–1604, Sep. 2003.

[4] S. J. Melby *et al.*, "Atrial fibrillation propagates through gaps in ablation lines: Implications for ablative treatment of atrial fibrillation," *Heart Rhythm*, vol. 5, no. 9, pp. 1296–1301, Sep. 2008.

[5] M. A. Miller *et al.*, "Acute electrical isolation is a necessary but insufficient endpoint for achieving durable PV isolation: The importance of closing the visual gap," *Europace*, vol. 14, no. 5, pp. 653–660, May 2012.

[6] R. Kobza *et al.*, "Late recurrent arrhythmias after ablation of atrial fibrillation: Incidence, mechanisms, and treatment," *Heart Rhythm*, vol. 1, no. 6, pp. 676–683, Dec. 2004.

[7] S. Nath and D. E. Haines, "Biophysics and pathology of catheter energy delivery systems," *Prog. Cardiovascular Diseases*, vol. 37, no. 4, pp. 185–204, Jan. 1995.

[8] L. L. Skrumeda and R. Mehra, "Comparison of standard and irrigated radiofrequency ablation in the canine ventricle," *J. Cardiovascular Electrophysiol.*, vol. 9, no. 11, pp. 1196–1205, Nov. 1998.

[9] D. C. Shah, H. Lambert, H. Nakagawa, A. Langenkamp, N. Aeby, and G. Leo, "Area under the real-time contact force curve (force–time integral) predicts radiofrequency lesion size in an *in vitro* contractile model," *J. Cardiovascular Electrophysiol.*, vol. 21, no. 9, pp. 1038–1043, Sep. 2010.

[10] A. Thiagalingam *et al.*, "Importance of catheter contact force during irrigated radiofrequency ablation: Evaluation in a porcine *ex vivo* model using a force-sensing catheter," *J. Cardiovascular Electrophysiol.*, vol. 21, no. 7, pp. 806–811, Jul. 2010.

[11] A. Kolandaivelu, M. M. Zviman, V. Castro, A. C. Lardo, R. D. Berger, and H. R. Halperin, "Noninvasive assessment of tissue heating during cardiac radiofrequency ablation using MRI thermography," *Circulat. Arrhythmia Electrophysiol.*, vol. 3, no. 5, pp. 521–529, Oct. 2010.

[12] T. Dickfeld *et al.*, "Characterization of radiofrequency ablation lesions with gadolinium-enhanced cardiovascular magnetic resonance imaging," *J. Amer. College Cardiol.*, vol. 47, no. 2, pp. 370–378, Jan. 2006.

[13] M. Wright *et al.*, "Real-time lesion assessment using a novel combined ultrasound and radiofrequency ablation catheter," *Heart Rhythm*, vol. 8, no. 2, pp. 304–312, Feb. 2011.

[14] M. Granier *et al.*, "Real-time atrial wall imaging during radiofrequency ablation in a porcine model," *Heart Rhythm*, vol. 12, no. 8, pp. 1827–1835, Aug. 2015.

[15] W. Kwiecinski *et al.*, "Validation of an intracardiac ultrasonic therapy–imaging dual mode transducer," *IRBM*, vol. 36, no. 6, pp. 351–354, Nov. 2015.

[16] W. Kwiecinski *et al.*, "Quantitative evaluation of atrial radio frequency ablation using intracardiac shear-wave elastography," *Med. Phys.*, vol. 41, no. 11, p. 112901, Nov. 2014.

[17] W. Kwiecinski *et al.*, "Cardiac shear-wave elastography using a transesophageal transducer: Application to the mapping of thermal lesions in ultrasound transesophageal cardiac ablation," *Phys. Med. Biol.*, vol. 60, no. 20, p. 7829, 2015.

[18] P. J. Hollender, P. D. Wolf, R. Goswami, and G. E. Trahey, "Intracardiac echocardiography measurement of dynamic myocardial stiffness with shear wave velocimetry," *Ultrasound Med. Biol.*, vol. 38, no. 7, pp. 1271–1283, Jul. 2012.

[19] S. A. Eyerly *et al.*, "Intracardiac acoustic radiation force impulse imaging: A novel imaging method for intraprocedural evaluation of radiofrequency ablation lesions," *Heart Rhythm*, vol. 9, no. 11, pp. 1855–1862, Nov. 2012.

[20] S. J. Hsu, B. J. Fahey, D. M. Dumont, P. D. Wolf, and G. E. Trahey, "Challenges and implementation of radiation-force imaging with an intracardiac ultrasound transducer," *IEEE Trans. Ultrason., Ferroelect., Freq. Control*, vol. 54, no. 5, pp. 996–1009, May 2007.

[21] J. Grondin, E. Wan, A. Gambhir, H. Garan, and E. E. Konofagou, "Intracardiac myocardial elastography in canines and humans *in vivo*," *IEEE Trans. Ultrason., Ferroelect., Freq. Control*, vol. 62, no. 2, pp. 337–349, Feb. 2015.

[22] Y. Yue, J. W. Clark, Jr., and D. S. Khoury, "Speckle tracking in intracardiac echocardiography for the assessment of myocardial deformation," *IEEE Trans. Biomed. Eng.*, vol. 56, no. 2, pp. 416–425, Feb. 2009.

[23] D. N. Stephens *et al.*, "Multifunctional catheters combining intracardiac ultrasound imaging and electrophysiology sensing," *IEEE Trans. Ultrason., Ferroelect., Freq. Control*, vol. 55, no. 7, pp. 1570–1581, Jul. 2008.

[24] J. Wang, S. Urheim, J. Korinek, T. P. Abraham, E. M. McMahon, and M. Belohlavek, "Analysis of postsystolic myocardial thickening work in selective myocardial layers during progressive myocardial ischemia," *J. Amer. Soc. Echocardiogr.*, vol. 19, no. 9, pp. 1102–1111, Sep. 2006.

[25] H. Chen, T. Varghese, P. S. Rahko, and J. A. Zagzebski, "Ultrasound frame rate requirements for cardiac elastography: Experimental and *in vivo* results," *Ultrasonics*, vol. 49, no. 1, pp. 98–111, Jan. 2009.

[26] E. A. Bunting, J. Provost, and E. E. Konofagou, "Stochastic precision analysis of 2D cardiac strain estimation *in vivo*," *Phys. Med. Biol.*, vol. 59, no. 22, p. 6841, Nov. 2014.

[27] J. Luo and E. E. Konofagou, "A fast normalized cross-correlation calculation method for motion estimation," *IEEE Trans. Ultrason., Ferroelect., Freq. Control*, vol. 57, no. 6, pp. 1347–1357, Jun. 2010.

[28] W. F. Walker and G. E. Trahey, "A fundamental limit on the performance of correlation based phase correction and flow estimation techniques," *IEEE Trans. Ultrason., Ferroelect., Freq. Control*, vol. 41, no. 5, pp. 644–654, Sep. 1994.

[29] C. Ma and T. Varghese, "Comparison of cardiac displacement and strain imaging using ultrasound radiofrequency and envelope signals," *Ultrasonics*, vol. 53, no. 3, pp. 782–792, Mar. 2013.

[30] W.-N. Lee, Z. Qian, C. L. Tosti, T. R. Brown, D. N. Metaxas, and E. E. Konofagou, "Preliminary validation of angle-independent myocardial elastography using MR tagging in a clinical setting," *Ultrasound Med. Biol.*, vol. 34, no. 12, pp. 1980–1997, Dec. 2008.

[31] W.-N. Lee, J. Provost, K. Fujikura, J. Wang, and E. E. Konofagou, "*In vivo* study of myocardial elastography under graded ischemia conditions," *Phys. Med. Biol.*, vol. 56, no. 4, p. 1155, Feb. 2011.

[32] E. Bunting, C. Papadacci, E. Wan, J. Grondin, and E. Konofagou, "Intracardiac myocardial elastography for lesion quantification in cardiac radiofrequency ablation," in *Proc. IEEE Int. Ultrason. Symp. (IUS)*, Sep. 2016, pp. 1–4.

[33] C. Papadacci, M. Pernot, M. Couade, M. Fink, and M. Tanter, "High-contrast ultrafast imaging of the heart," *IEEE Trans. Ultrason., Ferroelect., Freq. Control*, vol. 61, no. 2, pp. 288–301, Feb. 2014.

[34] G. Montaldo, M. Tanter, J. Bercoff, N. Benech, and M. Fink, "Coherent plane-wave compounding for very high frame rate ultrasonography and transient elastography," *IEEE Trans. Ultrason., Ferroelect., Freq. Control*, vol. 56, no. 3, pp. 489–506, Mar. 2009.

[35] C. Papadacci, E. A. Bunting, E. Y. Wan, P. Nauleau, and E. E. Konofagou, "3D myocardial elastography *in vivo*," *IEEE Trans. Med. Imag.*, vol. 36, no. 2, pp. 618–627, Feb. 2016.

[36] C. Papadacci, E. A. Bunting, and E. E. Konofagou, "3D quasi-static ultrasound elastography with plane wave *in vivo*," *IEEE Trans. Med. Imag.*, vol. 36, no. 2, pp. 357–365, Feb. 2017.

[37] D. Dausch, J. Castellucci, K. Gilchrist, J. Carlson, S. Hall, and O. von Ramm, "Real-time 3D intracardiac echo of the mitral valve using a novel live volumetric imaging catheter," *J. Amer. College Cardiol.*, vol. 61, no. 10, p. E1098, Mar. 2013.

[38] D. Wildes *et al.*, "4-D ICE: A 2-D array transducer with integrated ASIC in a 10-Fr catheter for real-time 3-D intracardiac echocardiography," *IEEE Trans. Ultrason., Ferroelect., Freq. Control*, vol. 63, no. 12, pp. 2159–2173, Dec. 2016.

Ethan Bunting was born in Wilmington, DE, USA. He received the B.S. degree in biomedical engineering from the University of Virginia, Charlottesville, VA, USA, in 2011. In 2011, he enrolled in the M.S./Ph.D. Program with the Department of Biomedical Engineering, Columbia University, New York, NY, USA.

He conducted his B.S. research with the Cardiac Biomechanics Group, where he focused on developing an imaging technique that could be used to accurately map the lead locations in patients with biventricular pacemakers. His senior design project involved the design of an artificial neural network algorithm that can be used by the emergency department to diagnose patients with STEMI. His current research interests include novel imaging techniques used to examine the electrical and mechanical activity of the heart, especially in diagnostic and clinical applications.

Clement Papadacci was born in Paris, France, in 1988. He received the Magistere degree in fundamental physics and the M.S. degree in acoustics from Paris VII University, Paris, in 2011, and the Ph.D. degree in physics from the Wave Physics for Medicine Team, Institut Langevin, Paris, in 2014.

He finished a Post-Doctoral Fellowship with the Ultrasound Elasticity Imaging Laboratory, as a Member of the Cardiac Team in 2016. He is currently an INSERM Researcher with the Wave Physics for Medicine Team, where he is in charge of clinical and preclinical studies. His current research interests include ultrafast elasticity imaging and 3-D ultrafast imaging of cardiovascular tissues.

Dr. Papadacci received several awards including the IEEE Student Award in 2013 and the Bettencourt Schueller Young Investigator Prize in 2015.

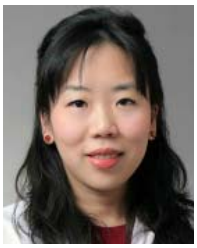

Elaine Wan received the bachelor's degree from the Massachusetts Institute of Technology, Cambridge, MA, USA, and the M.D. degree from Columbia University College of Physicians and Surgeons, New York, NY, USA. She completed her fellowship in cardiovascular diseases and clinical cardiac electrophysiology at New York Presbyterian/Columbia.

She is the Esther Aboodi Assistant Professor of Medicine in Cardiology and Cardiac Electrophysiology with Columbia University Medical Center, Columbia University College of Physicians and Surgeons, and an Attending Physician with the New York–Presbyterian Hospital, New York, NY, USA. She is a Physician–Scientist and a Translational Researcher focused on vascular ion channels and the development of innovative imaging modalities to improve ablation delivery.

Vincent Sayseng received the B.S. degree in biomedical engineering from the University of Rochester, Rochester, NY, USA, in 2014.

Since 2014, he has been a Biomedical Engineering Student of the M.S./Ph.D. Program with Columbia University, New York, NY, USA. His current research interests include ultrasound imaging to characterize the electrical and mechanical behavior of the heart in a noninvasive fashion.

Julien Grondin was born in Saint-Denis, Reunion Island, France, in 1983. He received the M.S. degree from Paris Diderot University (University of Paris VII), Paris, France, in 2007, and the Ph.D. degree from Pierre and Marie Curie University (University of Paris VI), Paris, in 2010.

In 2011, he joined the Ultrasound and Elasticity Imaging Laboratory, Columbia University, New York, NY, USA, as a Post-Doctoral Research Scientist, where he is currently an Associate Research Scientist with the Department of Biomedical Engineering. His research interests included ultrasonic characterization of bone properties. His current research interests include cardiac ultrasound imaging, myocardial elastography, and high-intensity focused ultrasound ablation monitoring.

Elisa E. Konofagou (S'98–A'99–M'03) is currently the Robert and Margaret Hariri Professor of biomedical engineering and a Professor of radiology as well as the Director of the Ultrasound and Elasticity Imaging Laboratory with the Biomedical Engineering Department, Columbia University, New York, NY, USA. She has co-authored over 170 peer-reviewed journal articles. Her current research interests include the development of novel elasticity imaging techniques and therapeutic ultrasound methods and more notably, myocardial elastography, electromechanical and pulse wave imaging, harmonic motion imaging, focused ultrasound therapy, and drug delivery in the brain, with several clinical collaborations in the Columbia Presbyterian Medical Center, New York, NY, USA, and elsewhere.

Prof. Konofagou was a recipient of awards, such as the CAREER Award from the National Science Foundation and the Nagy Award from the National Institutes of Health as well as others from the American Heart Association, the Acoustical Society of America, the American Institute of Ultrasound in Medicine, the Wallace H. Coulter Foundation, the Bodossaki Foundation, the Society of Photo-Optical Instrumentation Engineers, and the Radiological Society of North America. She is a Technical Committee Member of the Acoustical Society of America, the International Society of Therapeutic Ultrasound, the IEEE Engineering in Medicine and Biology Conference, the IEEE International Ultrasonics Symposium, and the American Association of Physicists in Medicine. She serves as an Associate Editor for the IEEE TRANSACTIONS ON ULTRASONICS, FERROELECTRICS, AND FREQUENCY CONTROL, *Ultrasonic Imaging*, and *Medical Physics*.